Biochimie 95 (2013) 382–387

Contents lists available at SciVerse ScienceDirect

Biochimie

journal homepage: www.elsevier.com/locate/biochi

Research paper

Maintenance and thermal stabilization of NADH dehydrogenase-2 conformation upon elimination of its C-terminal region

Josefina María Villegas [a], Clarisa María Torres-Bugeau [a], Rosana Chehín [a], Martha Inés Burgos [b], Gerardo Daniel Fidelio [b], María Regina Rintoul [a], Viviana Andrea Rapisarda [a,*]

[a] Instituto Superior de Investigaciones Biológicas (Consejo Nacional de Investigaciones Científicas y Técnicas-Universidad Nacional de Tucumán), and Instituto de Química Biológica "Dr Bernabé Bloj" (Universidad Nacional de Tucumán), Chacabuco 461, San Miguel de Tucumán T4000ILI, Argentina

[b] Departamento de Química Biológica, Centro de Investigaciones en Química Biológica de Córdoba (CIQUIBIC), UNC, Facultad de Ciencias Químicas, Pabellón Argentina – Ciudad Universitaria X5000HUA, Argentina

ARTICLE INFO

Article history:
Received 20 July 2012
Accepted 13 October 2012
Available online 23 October 2012

Keywords:
NDH-2
FAD
Truncated protein
Secondary structure
Protein thermal stability

ABSTRACT

Development of an artificial enzyme with activity and structure comparable to that of natural enzymes is an important goal in biological chemistry. Respiratory NADH dehydrogenase-2 (NDH-2) of *Escherichia coli* is a peripheral membrane-bound flavoprotein, belonging to a group of enzymes with scarce structural information. By eliminating the C-terminal region of NDH-2, a water soluble version with significant enzymatic activity was previously obtained. Here, NDH-2 structural features were established, in comparison to those of the truncated version. Far-UV circular dichroism, Fourier transform infrared spectroscopy and limited proteolysis analysis showed that the overall structure of both proteins was similar at 30 °C. Experimental data agree with the predicted NDH-2 structure (PDB: 1OZK). The absence of C-terminal region stabilized in ~5–10 °C the truncated protein conformation. However, truncation impaired enzymatic activity at low temperatures, probably due to the weak interaction of the mutant protein with FAD cofactor.

1. Introduction

Type II NADH dehydrogenase (NDH-2) is a member of the pyridine nucleotide disulfide reductases (PNDR) protein family that catalyzes the electron transfer from NADH to quinones without energy transduction [1,2]. NDH-2s are membrane-bound flavoproteins found in a broad range of organisms including plants, fungi, protozoa, and bacteria [3–5]. These enzymes have been proposed either as chemotherapeutic targets against pathogens or as complex I substitute in human gene therapy [6–9].

Respiratory NDH-2 of *Escherichia coli* has been biochemically characterized [10,11]. It consists of a single polypeptidic chain of 433 residues (47,200 Da), containing a non-covalently bound FAD as a redox cofactor [11]. 3D-model is restricted to theoretical studies based on sequence similarity using the flavoenzyme NAD(P)H peroxidase as template [12]. Also, several controversial models of how the enzyme is attached to the membrane have been described [2,12,13]. As a first experimental approach to specify the nature of the protein membrane interaction, we have recently reported that NDH-2 is a peripheral membrane protein, interacting with the membrane by at least a C-terminal amphipathic α-helix [14].

Based on these results, a water soluble NDH-2, named Trun-3, has been obtained by deletion of the C-terminal region [14]. Purified Trun-3 lacked FAD, rendering the enzyme inactive. The cofactor addition to the apoenzyme was necessary to restore Trun-3 activity. Studies have shown that Trun-3 and NDH-2 kinetics parameters were similar.

Trun-3 cytosolic nature offers a number of advantages, such as: time reduction and yield enhancement in the purification protocol; absence of detergent during the purification and storage; and increase of enzyme stability to freeze–thaw cycles.

In this work, we demonstrated that the overall structure of the truncated protein resembles the wild-type. Since the elimination of the C-terminal region apparently does not affect the globularity of NDH-2, Trun-3 could be an interesting tool for further structural characterizations of the enzyme. The absence of the C-terminal region contributes to the protein thermal stability. However, the mentioned region may stabilized the FAD binding in NDH-2, as seen by the decrease of Trun-3 activity at lower temperatures in respect to that of wild type protein.

* Corresponding author. Tel./fax: +54 381 4248921.
E-mail address: vrapisarda@fbqf.unt.edu.ar (V.A. Rapisarda).

0300-9084/$ – see front matter © 2012 Elsevier Masson SAS. All rights reserved.
http://dx.doi.org/10.1016/j.biochi.2012.10.010

2. Materials and methods

2.1. Chemicals and media

All chemicals and media were purchased from Sigma–Aldrich (St. Louis, MO, USA).

2.2. Protein expression and purification

Expression of His-tagged NDH-2 and Trun-3 proteins was induced with 0.1 mM IPTG in early log phase cultures of BLNdh and BLTrun-3 strains, respectively [14]. Both proteins were purified by affinity chromatography using a Ni-NTA column following the protocol adapted by Villegas et al. [14]. Protein concentration was determined by the method of Lowry et al. [15]. All structural assays were performed in 50 mM potassium phosphate buffer, pH 7.5, and 0.5 M NaCl, in the presence of a 4-fold molar excess of FAD.

2.3. Circular dichroism

Far-UV circular dichroism (CD) spectra were performed on a Jasco 810 spectropolarimeter under constant N_2 flush, equipped with a Haake temperature control unit. Scans were carried out in a 2 mm path length quartz cuvette at a speed of 100 nm min^{-1}, a band width of 1 nm, a data pitch of 0.2 nm s^{-1} and a response time of 1 s. Buffer scans were subtracted from the proteins spectra. The results were expressed as mean residual ellipticity [θ], given in deg cm^2 $dmol^{-1}$ [16].

2.4. Fourier transform infrared spectroscopy

Lyophilized NDH-2 or Trun-3 samples (5 mg ml^{-1}) were resuspended in D_2O. Spectra were recorded in Nicolet 5700 spectrometer equipped with a DTGS detector (Thermo Nicolet, Madison, WI) in thermostated cell between two CaF_2 windows. The sample chamber was permanently purged with dry air to reduce distortions of water-vapor. Scans were collected at a nominal resolution of 2 cm^{-1} and apodized with a Happ–Genzel function. Solvent subtraction, deconvolution, determination of band position and curve fitting of the original amide I band were performed as described [17]. The error in estimation of the percentage of secondary structure depends mainly on the removal of spectral noise, and it was estimated to be 2–3% [18].

2.5. Limited proteolysis

Samples (0.5 mg ml^{-1}) were incubated with bovine pancreas chymotrypsin at 30 °C (protease/protein ratio 1:30). Reaction was stopped after 1 h by adding SDS-PAGE loading buffer and boiling at 100 °C for 5 min. Proteolysis reaction products were analyzed by 10% SDS-PAGE [19], and stained with Colloidal Coomassie Blue. A ~42 kDa proteolytic band was then excised and sequenced (CEQUIBIEM, Argentina).

2.6. Activity assays

NADH dehydrogenase activity was measured as reported by Rapisarda et al. [20]. Briefly, NADH oxidation was followed by absorbance decrease at 340 nm using duroquinone (Q_0) as electron acceptor. It is worth to mention that in this case, 10 μM FAD was added to the reaction mixture.

2.7. Differential scanning calorimetry

Calorimetric experiments were obtained using a MicroCal VP-DSC calorimeter from MicroCal Llc. (Northampton, MA, USA). The protein concentration was 0.5 mg ml^{-1}. All the solutions were degassed. The reference cell was filled with buffer and a pressure of 26 p.s.i. was applied to both cells. A scan rate of 60 °C/h was used in all experiments. Buffer–buffer scan was subtracted to the crude sample scan and subsequently normalized for total protein concentration. The experimental data were deconvoluted using Origin software provided by the manufacturer. A non two-state transition analysis was applied, previous baseline subtraction, to obtain the thermal transition mid-point (T_m).

2.8. Fluorescence spectroscopy

Measurements of intrinsic fluorescence were carried out on a PerkinElmer Life Sciences LS50 fluorimeter equipped with a thermostated cell holder. All experiments were performed following an excitation wavelength of 295 nm, known to be specific for tryptophan (Trp). Fluorescence emission was scanned from 300 to 450 nm. Sample solutions were prepared at a protein concentration of 0.2 mg ml^{-1}.

3. Results

3.1. Comparison of Trun-3 and NDH-2 structural features

There is scarce structural information yet on any type II NADH oxidoreductase. Structural model is restricted to theoretical studies based on sequence similarity with other flavoenzymes used as templates such as the lipoamide dehydrogenases and NAD(P)H peroxidases [12,21]. 3D-model for *E. coli* NDH-2 comprises 385 amino acid residues, since the last C-terminal residues were not located in detail due to ambiguities in the alignment [12]. Here, *E. coli* NDH-2 structural features were studied by different techniques, such as circular dichroism (CD), Fourier transform infrared spectroscopy (FTIR), fluorescence spectroscopy and limited proteolysis. Structural studies were also performed with Trun-3, a soluble variant that mimics the modeled fragment, in order to investigate similarities to wild type enzyme and to corroborate bioinformatics data.

Far-UV CD spectra were used to estimate the secondary structure of wild-type and Trun-3. Both proteins presented a characteristic α/β spectrum at 30 °C (Fig. 1A). As observed, spectra did not reveal any major difference, indicating that the conformation adopted by the two proteins were similar. Infrared spectroscopy analyses were also performed in order to compare secondary structure contents. Fig. 1B and C shows NDH-2 and Trun-3 deconvoluted amide I spectra at 30 °C. The band at ~1654 cm^{-1} reflects the α-helices content while the band component at ~1632 cm^{-1} indicates the β-sheet fraction. The band located around 1665 cm^{-1} corresponds to β-turns. The band at 1675 cm^{-1} indicates a small contribution of the high-frequency vibration of the antiparallel β-strands. Bands at about 1642 cm^{-1} are assigned to non-structured conformation. On the basis of the mentioned assignments, NDH-2 contains 28% α-helix, 20% β-sheets, and 16% β-turns, while Trun-3 structure consists of 20% α-helix, 26% β-sheets, and 19% β-turns (Table 1).

Both proteins have two tryptophan residues at positions 46 and 272. When NDH-2 intrinsic tryptophan fluorescence was monitored at 30 °C, an emission peak centered at 345 nm was observed, while the Trp emission maximum of Trun-3 was around 4-nm blue-shifted in respect to that of the native protein (data not shown).

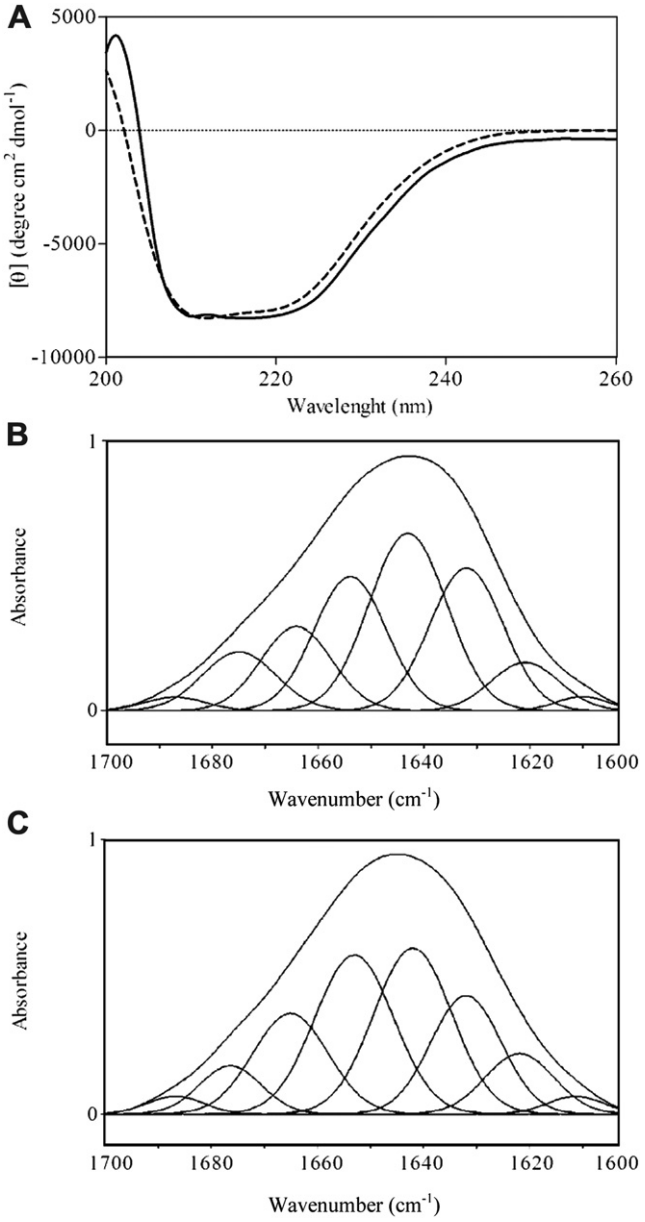

Fig. 1. Far-UV CD and FTIR spectra. (A) NDH-2 (black line) and Trun-3 (dashed line) far-UV CD spectra at 30 °C. Data are expressed as mean molar residue ellipticity [θ]. Each CD spectrum was the average of five scans. (B) Trun-3 and (C) NDH-2 FTIR amide I band deconvolution at 30 °C. FTIR spectra were the average of 16 scans. CD and FTIR experiments were repeated three times and performed in the presence of 4-fold molar excess of FAD.

Table 1
FTIR band position and percentage area corresponding to the components obtained after curve fitting of Trun-3 and NDH-2 amide I band at 30 °C.

Trun-3		NDH-2	
Position (cm^{-1})	Area (%)	Position (cm^{-1})	Area (%)
1611	2	1611	2
1622	5	1622	7
1632	26	1632	20
1644	23	1642	21
1654	20	1652	28
1665	19	1665	16
1675	3	1676	4
1686	2	1687	2

When NDH-2 chymotryptic digestion was carried out, a major 42 kDa product was observed at 15 min and 1 h of treatment, similar in mass to Trun-3 (Fig. 2, lane 4 and 6). This fragment lacked C-terminal region, as confirmed by sequence analysis. Besides, comparable digestion band profiles were seen for both proteins till 1 h of treatment (Fig. 2, lane 4–7). After 2:30 h, wild-type protein was more prone to degradation than the mutant version (Fig. 2, lane 8 and 9).

3.2. NDH-2 and Trun-3 thermal profiles

The effect of increasing temperature on NDH-2 and Trun-3 activity was investigated. As reported in Fig. 3, Trun-3 enzymatic activity progressively decreased from 20 °C, whereas the wild-type protein activity drastically declined after 34 °C. Both proteins were almost inactive from 41 °C.

Thermal transition curves of NDH-2 and Trun-3 were followed by CD intensity at 222 nm, which reflect α-helices content (Fig. 4A). No significant changes were observed in CD ellipticity at 222 nm up to 41 °C, although both enzymes activity were lost at this temperature. For NDH-2, loss of secondary structure occurred over a range from 43 to 50 °C, and the apparent midpoint transition temperature (T_m) was 44.8 °C. For Trun-3, these changes occurred between 45 and 55 °C, with a T_m of 48.9 °C. Thermal profiles were further analyzed by plotting the full-width at half height of FTIR amide I band as a function of temperature (Fig. 4B). Loss of secondary structure in NDH-2 occurred within a range from 45 to 50 °C with a T_m of 47 °C, while for Trun-3 was between ~47 and 55 °C, with a T_m of 50 °C. From the deconvolution analysis of amide I band at increasing temperatures (data not shown), it was observed that α-helix content decreased (mainly in NDH-2), whereas the bands related to random coil and β-sheets increased. Simultaneously, a shift to higher wavelengths in the band at ~1654 cm^{-1} occurred, demonstrating an α-helix distortion. Taken together, these data are indicative of protein unfolding and aggregation processes.

To further characterize the thermal transitions of NDH-2 and Trun-3, high-sensitivity differential scanning calorimetry (DSC) measurements were carried out. As shown in Fig. 5, the heat flow profile versus temperature contained several endothermic peaks, suggesting that the thermal unfolding of both proteins contained stepwise transitions. Both calorimetric scans consisted of three entities melting at different temperatures. The lower transition peak for NDH-2 had a T_m of 36.8. The other peaks were located at 42.3 and 44.7 °C, being the last one the higher transition peak (Fig. 5A and Table 2). On the other hand, Trun-3 presented transition peaks at 43.8, 50.4 and 53 °C (Fig. 5B and Table 2). It is worth to mention that for both proteins, the endothermic unfolding transition was followed by an abrupt exothermic transition (data not shown). This led to an uncertain baseline correction and,

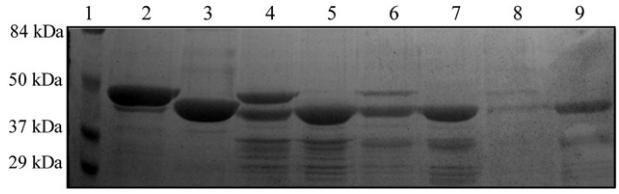

Fig. 2. Limited proteolysis with chymotrypsin. 10% SDS-PAGE of NDH-2 and Trun-3 chymotryptic products. Samples were incubated in the presence of 4-fold molar excess of FAD for 1 h at 30 °C. Gel was stained with Colloidal Coomassie Blue. Lane 1: Low range prestained SDS-PAGE standards (BIO-RAD); lane 2: NDH-2 before digestion; lane 3: Trun-3 before digestion; lane 4–9: NDH-2 and Trun-3 after 15 min, 1 h and 2:30 h digestion, respectively. Representative results from three sets of experiments are shown.

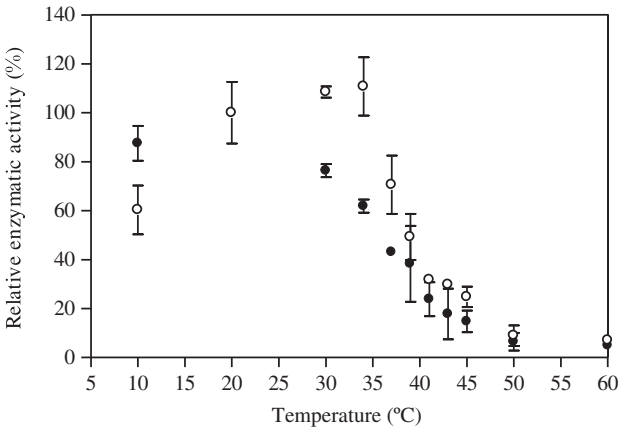

Fig. 3. Thermal profile of enzymatic activity. NADH:quinone oxidoreductase activity of NDH-2 (open circles) and Trun-3 (filled circles) measured in the presence of 10 μM FAD. For each protein, data were normalized by the enzymatic activity at 20 °C.

therefore, a rigorous thermodynamic analysis could not be performed.

Temperature transition curves monitoring tryptophan-fluorescence emission were also studied. Fig. 6 shows at least two transitions: a change in the intensity at 41 and 45 °C for NDH-2 and Trun-3, respectively, followed by a major breakpoint at 55 °C, from

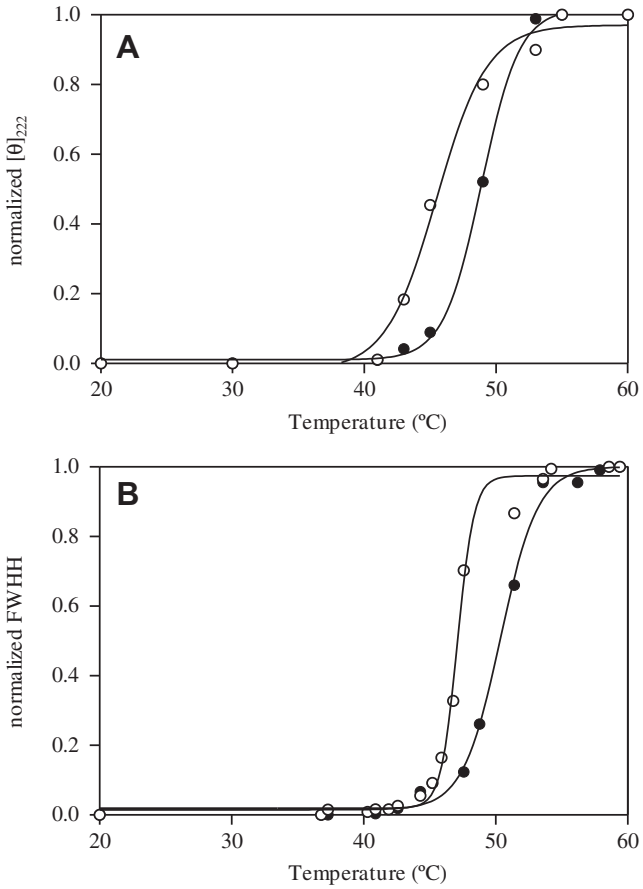

Fig. 4. Thermal transition curves by far-UV CD and FTIR. Temperature dependence of spectroscopic signals for NDH-2 (open circles) and Trun-3 (filled circles). Values are relative to the total change observed between 20 and 60 °C, following (A) ellipticity at 222 nm by CD and (B) full-width at half-height of the amide I band by FTIR. Experiments were carried out upon addition of 4-fold molar excess of FAD.

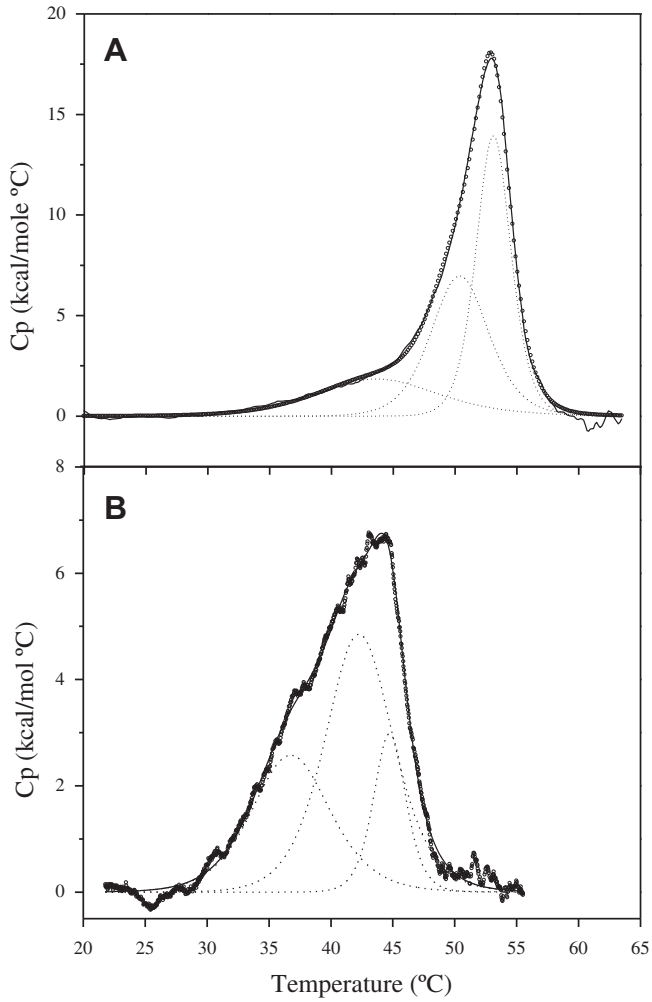

Fig. 5. Differential scanning calorimetry thermograms. (A) Trun-3 and (B) NDH-2 DSC experimental data points (circles), best fit curves (solid line) and transitions obtained from the non-two-state transition model analyses (dotted lines) are shown. Crude thermograms were normalized by total protein concentration. Samples were incubated with FAD (protein:FAD 1:4).

where the intensity started to decrease in both cases. Unfolding at 60–70 °C was marked by a red shift to ~346 nm for both proteins (data not shown).

4. Discussion

For the first time, we were able to experimentally establish NDH-2 structural features and compared to those of its soluble variant, Trun-3. Experimental data obtained by the different

Table 2
Thermal transition mid-points of Trun-3 and NDH-2 as determined by different approaches.

	Trun-3	NDH-2
	T_m (°C)	
DSC	43.8	36.8
	50.4	42.3
	53	44.7
Trp fluorescence	45	41
	55	55
Far-UV CD	48.5	45
FTIR	50	47

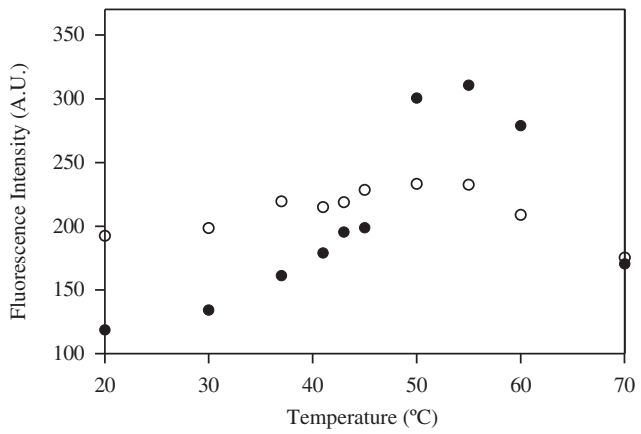

Fig. 6. Effects of thermal treatment on tryptophan fluorescence intensity. Spectra were collected with excitation wavelength at 295 nm. Experiments were performed in the presence of 4-fold molar excess of FAD. Values correspond to NDH-2 (open circles) and Trun-3 (filled circles) maximal fluorescence intensity as averages between 335 and 355 nm.

techniques agree with NDH-2 structure predicted by Schmid and Gerloff (PDB: 1OZK) [12]. Both proteins have similar secondary structure profiles, as observed by far-UV CD. Due to the limited resolution of this technique, complementary data by infrared spectroscopy were appropriate [22]. FTIR analyses showed that Trun-3 had 8% less α-helices content compared to NDH-2. This is in agreement with the fact that 33 aminoacids predicted to form two C-terminal amphipathic helices are absent in Trun-3 [12,14]. Since the FTIR assignations are expressed as relative values, the decrease in α-helices content resulted in a larger β-sheets fraction. By analyzing the PDB file with Visual Molecular Dynamics (VMD) program [23], solvent-accessible surface area (SASA) was calculated for Trp-46 and Trp-272, obtaining values of 33.5 and 8.96 Å, respectively. This indicates that both tryptophan residues are partially buried to the solvent, compatible with the wavelengths of maximum tryptophan fluorescence emission obtained for NDH-2 and Trun-3. However, intrinsic fluorescence revealed subtle differences between both enzymes, indicating that at least one of the tryptophan moieties in the truncated protein is surrounded by a slightly more hydrophobic microenvironment [24]. This fluorescence change may be due to the FAD cofactor that could be closer to Trp in Trun-3 than in NDH-2. Further, limited proteolysis experiments showed a similar fragmentation pattern between both proteins, indicating a comparable conformation. Taken together, we consider that the elimination of C-terminal region would not affect NDH-2 globularity, since no significant differences in the overall topology of both proteins were observed. These data, complemented with the similar K_m values obtained in previous biochemical characterization [14], allow us to propose that the substrate binding site(s) of both enzymes remained unchanged.

Both proteins suffered functional/conformational changes when the temperature increased, including loss of enzymatic activity, alteration of tertiary structure, loss of some secondary structure elements and unfolding with aggregation. For NDH-2, changes in intrinsic fluorescence and DSC measurements, reflecting modifications in tertiary structure, occurred within the temperature range in which activity decreased. On the other hand, Trun-3 enzymatic activity decreased over a broader temperature range and it was lost prior to any detectable structural change. This gradual drop of activity may be related to the weak interaction between Trun-3 and FAD [14]. For NDH-2 and Trun-3, changes in tertiary structure preceded the major change in secondary structure. Interestingly, modifications in secondary structure occurred at temperatures that agree with the second transition seen by DSC. At 60–70 °C, a disorder of the overall proteins structure was observed, denoted by an exposure of buried tryptophan residues toward the solvent as seen by fluorescence spectroscopy. This thermal unfolding was also observed by DSC, where a sharp exothermic transition followed the endothermic transition in both proteins. In IR spectra, characteristic bands at 1611 and 1687 cm^{-1} became significant at these temperatures. These DSC and IR phenomena are indicative of protein aggregation [17,25].

An interesting finding from this study is that midpoint transition temperatures, detected by various experimental techniques, were approximately 5–10 °C higher for the truncated version than for NDH-2, indicating that the absence of C-terminal region increased the structural stability of Trun-3 toward increasing temperatures. As observed by FTIR, the early unfolding events occurred through α-helices, probably leading to a destabilization of the C-terminal region that seems to be more flexible and susceptible to temperature changes. Also, short-times limited digestion of NDH-2 produced a fragment lacking C-terminal region, supporting the proposed instability of this region. It should be considered that NDH-2 natural environment is the membrane, which can contribute to the enzyme stability by the attachment of its amphipathic helix. It has been demonstrated that NDH-2 activity was improved by pre-incubation in the presence of phospholipids [26].

The absence of C-terminal region impaired the enzyme ability to maintain the cofactor bound [14], which could explain the fact that Trun-3 enzymatic activity profile did not agree with its higher structural stability. Moreover, temperature caused a more abrupt tryptophan fluorescence change in Trun-3 than in wild type, which is in agreement with the weak interaction of FAD and Trun-3. In other flavoproteins, increasing temperatures produce break down of flavin interactions, usually leading to large increase in intrinsic fluorescence [27].

In conclusion, the overall structure of Trun-3 resembles the wild-type protein, and the absence of C-terminal region contributes to the protein thermal stability. However, the decrease of Trun-3 activity indicates that the C-terminal region improves enzymatic activity at low temperatures, possibly by a stabilization of FAD binding. A broad knowledge about NDH-2 enzymes could promote their potential applications in medical science and biotechnology.

Acknowledgments

We specially thank Dr. Fernando G. Dupuy for helpful discussion. This research was supported by grants 26/D329 from CIUNT, PIP6399 from CONICET. J. M. V. and C. T. B. are pre-doctoral fellows of CONICET (Argentina).

References

[1] C.L. Ávila, V.A. Rapisarda, R.N. Farías, J. De Las Rivas, R. Chehín, Linear array of conserved sequence motifs to discriminate protein subfamilies: study on pyridine nucleotide-disulfide reductases, BMC Bioinform. 8 (2007) 96.
[2] A.M. Melo, T.M. Bandeiras, M. Teixeira, New insights into type II NAD(P)H: quinone oxidoreductases, Microbiol. Mol. Biol. Rev. 68 (2004) 603–616.
[3] J. Fang, D.S. Beattie, Novel FMN-containing rotenone-insensitive NADH dehydrogenase from *Trypanosoma brucei* mitochondria: isolation and characterization, Biochemistry 41 (2002) 3065–3072.
[4] A.M. Michalecka, A.S. Svensson, F.I. Johansson, S.C. Agius, U. Johanson, A. Brennicke, S. Binder, A.G. Rasmusson, Arabidopsis genes encoding mitochondrial type II NAD(P)H dehydrogenases have different evolutionary origin and show distinct responses to light, Plant Physiol. 133 (2003) 642–652.
[5] M.G. Matus-Ortega, K.G. Salmerón-Santiago, O. Flores-Herrera, G. Guerra-Sánchez, F. Martínez, J.L. Rendón, J.P. Pardo, The alternative NADH dehydrogenase is present in mitochondria of some animal taxa, Comp. Biochem. Physiol. Part. D Genom. Proteomics 6 (2011) 256–263.
[6] G.A. Biagini, P. Viriyavejakul, P.M. O'neill, P.G. Bray, S.A. Ward, Functional characterization and target validation of alternative complex I of *Plasmodium*

falciparum mitochondria, Antimicrob. Agents Chemother. 50 (2006) 1841–1851.

[7] A. Saleh, J. Friesen, S. Baumeister, U. Gross, W. Bohne, Growth inhibition of Toxoplasma gondii and Plasmodium falciparum by nanomolar concentrations of HDQ (1-hydroxy-2-dodecyl-4(1H)quinolone): a high affinity inhibitor of alternative (type II) NADH dehydrogenases, Antimicrob. Agents Chemother. 51 (2007) 1217–1222.

[8] T. Yagi, B.B. Seo, E. Nakamaru-Ogiso, M. Marella, J. Barber-Singh, T. Yamashita, A. Matsuno-Yagi, Possibility of transkingdom gene therapy for complex I diseases, Biochim. Biophys. Acta 1757 (2006) 708–714.

[9] M. Marella, B.B. Seo, T. Yagi, A. Matsuno-Yagi, Parkinson's disease and mitochondrial complex I: a perspective on the Ndi1 therapy, J. Bioenerg. Biomembr. 41 (2009) 493–497.

[10] I.G. Young, B.L. Rogers, H.D. Campbell, A. Jaworowski, D.C. Shaw, Nucleotide sequence coding for the respiratory NADH dehydrogenase of *Escherichia coli*: UUG initiation codon, Eur. J. Biochem. 116 (1981) 165–170.

[11] A. Jaworowski, G. Mayo, D.C. Shaw, H.D. Campbell, I.G. Young, Characterization of the respiratory NADH dehydrogenase of *Escherichia coli* and reconstitution of NADH oxidase in ndh mutant membrane vesicles, Biochemistry 20 (1981) 3621–3628.

[12] R. Schmid, D.L. Gerloff, Functional properties of the alternative NADH: ubiquinone oxidoreductase from *E. coli* through comparative 3-D modeling, FEBS Lett. 578 (2004) 163–168.

[13] V.A. Rapisarda, R.N. Chehín, J. De Las Rivas, L. Rodríguez-Montelongo, R.N. Farías, E.M. Massa, Evidence for Cu(I)-thiolate ligation and prediction of a putative copper-binding site in the *Escherichia coli* NADH dehydrogenase-2, Arch. Biochem. Biophys. 405 (2002) 87–94.

[14] J.M. Villegas, S.I. Volentini, M.R. Rintoul, V.A. Rapisarda, Amphipathic C-terminal region of *Escherichia coli* NADH dehydrogenase-2 mediates membrane localization, Arch. Biochem. Biophys. 505 (2011) 155–159.

[15] O.H. Lowry, N.J. Rosebrough, A.L. Farr, R.J. Randall, Protein measurement with the Folin phenol reagent, J. Biol. Chem. 193 (1951) 265–275.

[16] J.B. Bertoldo, G. Razzera, J. Vernal, F.C. Brod, A.C. Arisi, H. Terenzi, Structural stability of *Staphylococcus xylosus* lipase is modulated by Zn(2+) ions, Biochim. Biophys. Acta 1814 (2011) 1120–1126.

[17] J.L. Arrondo, J. Castresana, J.M. Valpuesta, F.M. Goñi, Structure and thermal denaturation of crystalline and noncrystalline cytochrome oxidase as studied by infrared spectroscopy, Biochemistry 33 (1994) 11650–11655.

[18] I. Echabe, J.A. Encinar, J.L.R. Arrondo, Removal of spectral noise in the quantitation of protein structure through infrared band decomposition, Biospectroscopy 3 (1997) 469–475.

[19] U.K. Laemmli, Cleavage of structural proteins during the assembly of the head of bacteriophage T4, Nature 227 (1970) 680–685.

[20] V.A. Rapisarda, L.R. Montelongo, R.N. Farías, E.M. Massa, Characterization of an NADH-linked cupric reductase activity from the *Escherichia coli* respiratory chain, Arch. Biochem. Biophys. 370 (1999) 143–150.

[21] N. Fisher, A.J. Warman, S.A. Ward, G.A. Biagini, Chapter 17 Type II NADH: quinone oxidoreductases of *Plasmodium falciparum* and *Mycobacterium tuberculosis* kinetic and high-throughput assays, Methods Enzymol. 456 (2009) 303–320.

[22] M. Calero, M. Gasset, Fourier transform infrared and circular dichroism spectroscopies for amyloid studies, Methods Mol. Biol. 299 (2005) 129–151.

[23] W. Humphrey, A. Dalke, K. Schulten, VMD-visual molecular dynamics, J. Molec. Graphics 14 (1) (1996) 33–38.

[24] J.R. Lakowicz, Principles of Fluorescence Spectroscopy, third ed., Plenum Press, New York, USA, 2006.

[25] S. D'auria, R. Barone, M. Rossi, R. Nucci, G. Barone, D. Fessas, E. Bertoli, F. Tanfani, Effects of temperature and SDS on the structure of beta-glycosidase from the thermophilic archaeon *Sulfolobus solfataricus*, Biochem. J. 323 (1997) 833–840.

[26] K. Bjorklof, V. Zickermann, M. Finel, Purification of the 45 kDa, membrane bound NADH dehydrogenase of Escherichia coli (NDH-2) and analysis of its interaction with ubiquinone analogues, FEBS Lett. 467 (2000) 105–110.

[27] A.W. Munro, M.A. Noble, Fluorescence analysis of flavoproteins. Flavoprotein protocols, Methods Mol. Biol. 131 (1999) 25–48.